DOI: 10.1002/smll.200700148

Specific Integrin Labeling in Living Cells Using Functionalized Nanocrystals

*Oliver Lieleg, Mónica López-García, Christine Semmrich, Jörg Auernheimer, Horst Kessler, and Andreas R. Bausch**

***W**e present an integrin labeling method using functionalized quantum dots (QDs). Cyclic Arg-Gly-Asp (RGD) peptides and a biotin–streptavidin linkage are used to specifically couple individual QDs to integrins of living cells. The spacer distance between the RGD sequence and the QD surface is a crucial parameter to ensure specific binding to individual $\alpha_v\beta_3$ integrins of osteoblast cells. Despite blinking, the position of single QDs is tracked with nanometer precision and localized diffusive behavior is observed. We show that blinking events do not prevent the acquisition of quantitative parameters from the QD trajectories.*

Keywords:
- bioimaging
- cells
- labeling
- peptides
- quantum dots

1. Introduction

Quantum dot (QD) bioimaging has recently been described as the most exciting new technique to emerge from the collaboration of physicists and biologists.[1] This new molecular imaging technology is based on the selective fluorescent labeling of biological molecules. QDs are fluorescent nanocrystals showing a wide-range absorption spectrum (400–650 nm) and a narrow, symmetric emission spectrum.[2] By choosing the appropriate QD size, the emission wavelength can be tuned even to the near infrared. This allows the QD signal to be clearly distinguished from the cell autofluorescence background. Finally, the stability of QDs against oxidation and photobleaching makes them highly suitable for single-molecule labeling compared to conventional dyes. Based on these unique spectral, physical, and chemical properties, QDs are extremely useful as a technique to "light up" biological events. However, besides all their advantages, QDs do not offer a continuous fluorescence signal as they exhibit a statistical blinking behavior. This feature hampers automated image processing and might adulterate the quantitative parameters that are extracted from the trajectories of such blinking particles.[3]

The possibility to visualize integrin expression and to analyze the interaction with specific ligands has great importance in basic biological studies. Integrins are heterodimeric transmembrane proteins composed of two noncovalently associated subunits (α and β).[4] The 18 α and 8 β subunits that are known can combine to form 24 different heterodimers, which differ in their ligand specificity.[5] These proteins represent the most numerous and versatile family of bidirectional transmembrane cell receptors, which regulate the cell–cell and cell–extracellular matrix (ECM) interactions in multicellular organisms.[6] These interactions influence many fundamental cellular functions, such as motility, proliferation, differentiation, and apoptosis.

The tripeptide sequence Arg-Gly-Asp (RGD) was identified as a minimal essential cell-adhesion peptide sequence in fibronectin.[7] Since then, cell-adhesive RGD motifs have been identified in many other ECM proteins, including vitronectin, fibrinogen, collagen, laminin, and osteopontin.

[*] O. Lieleg, C. Semmrich, Prof. A. R. Bausch
Lehrstuhl für Biophysik E22
Technische Universität München
James-Franck-Strasse 1, 85748 Garching (Germany)
Fax: (+49) 89-289-12469
E-mail: abausch@ph.tum.de
Dr. M. López-García, Dr. J. Auernheimer, Prof. H. Kessler
Lehrstuhl für Organische Chemie II
Technische Universität München
Lichtenbergstrasse 4, 85748 Garching (Germany)
Dr. J. Auernheimer
Klinikum rechts der Isar der Technischen Universität München
Nuklearmedizinische Klinik und Poliklinik
Ismaningerstrasse 22, 81675 München (Germany)

NANO MICRO small

About half of the 24 integrins have been shown to bind to ECM molecules in an RGD-dependent manner.[8] The RGD sequence is the most effective and often employed sequence to stimulate cell adhesion on synthetic surfaces.[9,10] This is based on its widespread distribution and use in the organism, its ability to address more than one cell-adhesion receptor, and its biological impact on cell anchoring, behavior, and survival. Suitable optimized cyclic RGD (cRGD) peptides[11] interact with integrin receptor subtypes in a more selective manner and with higher affinity than linear peptides. However, these positive effects of cyclization are only observed when the bioactive conformation is matched. In the case of RGD peptides, a "spatial screening" procedure was applied to optimize the structure–activity relationship.[12] Modification of the amino acid sequences flanking the RGD motif or changing its three-dimensional structure have been shown to modify the ligand selectivity.[11,13] Herein, the antagonist, cyclic pentapeptide cyclo(-RGDfK-), is employed as a specific integrin ligand.[14] The D-phenylalanine residue (f = D-Phe) following the RGD binding sequence is essential to enhance the α_v selectivity[12,15,16] versus the platelet receptor $\alpha_{IIb}\beta_3$ (to induce the preferred adhesion of osteoblasts rather than of platelets), and the lysine residue (K = Lys) allows the coupling of the RGD peptide to the spacer–anchor system.

Integrin-mediated cell adhesion to surfaces modified with specific ligands depends on many factors, such as affinity and specificity of the ligands to the particular integrin, spacer length, overall ligand concentration, surface topography, and ligand density. Therefore, not only the specific integrin ligand but also the anchor and the spacer should be considered in the optimization of the coating system.[11,17,18]

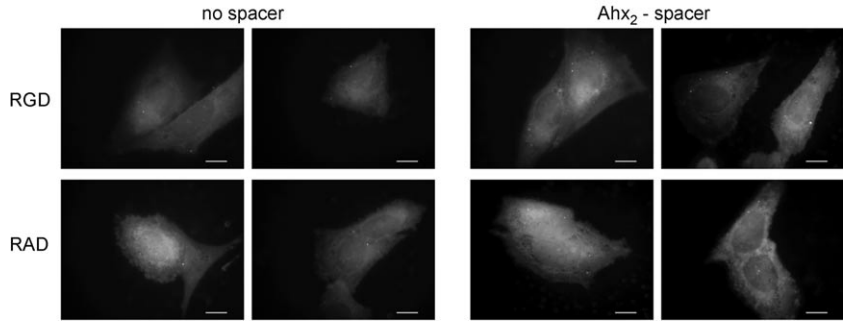

Figure 1. Constructs without spacer and with the short Ahx_2-spacer sequence. Both constructs do not show specific binding, as revealed by the control groups. The number of bound QDs is very low (only 2–5 QDs per cell). Scale bars: 10 μm. RAD: Arg-Ala-Asp.

2. Results and Discussion

First, constructs without a spacer are compared to the short Ahx_2-spacer constructs (Ahx: aminohexanoic acid). For both constructs the cyclo(-RβAGfK-) motif is used as negative control. As depicted in Figure 1, the number of bound QDs is very low (2–5 QDs per cell) for both groups as well as for the control molecules. From this result we conclude that specific binding of the RGD motif seems not to be possible for these spacer distances, and the few QDs observed bind due to unspecific interactions with the cell membrane. This finding is in agreement with former experiments of intervesicle cross-linking with integrins and cRGD lipopeptides,[19,20] for which a critical spacer distance necessary for the coupling of biotin constructs to streptavidin molecules was also reported. As the RGD-binding site of integrins is located in a deep cleft between the two integrin subunits,[21] a considerable part of the spacer is necessary to allow appropriate binding.

In fact, the use of long spacer constructs ($Hegas_2$, where Hegas is 20-amino-3,6,9,12,15,18-hexaoxaeicosanoic acid) dramatically affects the results. While the binding efficiency of the control-group constructs (this time using the cyclo(-RDGfK-) motif) is still very low, a highly enhanced binding of the cyclo(-RGDfK-) constructs can be observed (see Figure 2). The number of bound QDs per cell is increased

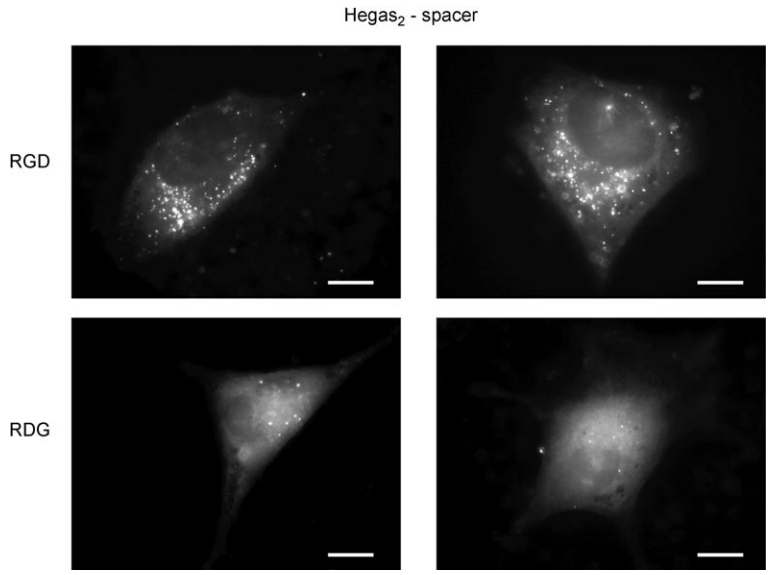

Figure 2. Constructs with the long $Hegas_2$ spacer show specific binding. The number of bound QDs per cell exceeds that of the control group by a factor of 50–100. Scale bars: 10 μm.

by a factor of 50–100 compared to that with shorter spacer distances.

For the cyclo(-RGDfK-) constructs, image processing is used to track the motion of single QDs.[3,22] Three qualitatively different types of trajectories are identified (see Figure 3C–E). Most of the QDs (>95%) are tightly bound and move only within an area of 40×40 nm, which meets the optical-resolution limit. Thus, we speculate that these QDs might cross-bridge several integrins, which is possible since the QD surface bears up to five streptavidin molecules per hemisphere. A second group of trajectories shows a motion similar to free diffusion. Nevertheless, the corresponding QDs do not freely float around in the medium but are weakly bound to the cell's surface. Most likely they are electrostatically trapped in the glycocalix, as they defocus from time to time and thus are not specifically bound at all. The third group reveals a localized diffusive motion similar to what is reported for membrane proteins.[23] In accordance with our hypothesis that most QDs might crosslink several integrins, these trajectories are observed only very rarely.

The observed label densities are much lower than the literature value for, for example, fibroblasts[24] but still seem to be reasonable if one considers that most of the integrins are collected on the bottom of the cell to build up points of focal adhesions. As the osteoblasts are incubated with the QD constructs after the formation of adhesion points, only the top part of the cell is accessible to our labeling, which results in a relatively low QD density. In addition, it was reported that oligomeric cRGD constructs show an increased affinity to α_v integrins, as their IC_{50} value (median inhibitory concentration) is a factor of 20–250 smaller than that of single cRGD molecules in vivo[25] and in vitro.[26–28] In principle, our functionalized QDs can be seen as oligomeric cRGD constructs, too. Thus, it seems reasonable to assume that during the rinsing step—after the cells have been incubated with the QD solution—QDs that are bound to a single integrin are predominantly washed off. This would reduce the absolute number of bound QDs per cell as well as the number of diffusion-like trajectories and thus would account for both observed effects.

While QDs are reported to be very stable against photobleaching, the lifetime of the QDs used in this study is limited. A drastic decrease in the total number of blinking QDs is observed over time, as after only 10 s of continuous illumination approximately 50% of the QDs have died down (see Figure 3B). Although it is hard to imagine how a semiconductor-based QD should be subjugated to chemical oxidation, this "photobleaching" has been reported before[3,29,30] and prevents us from following the QD motion over long periods. Therefore, the acquisition of tracking data is limited to short times, thus preventing the extraction of quantitative parameters, such as diffusion constants, since they rely on adequate statistics.

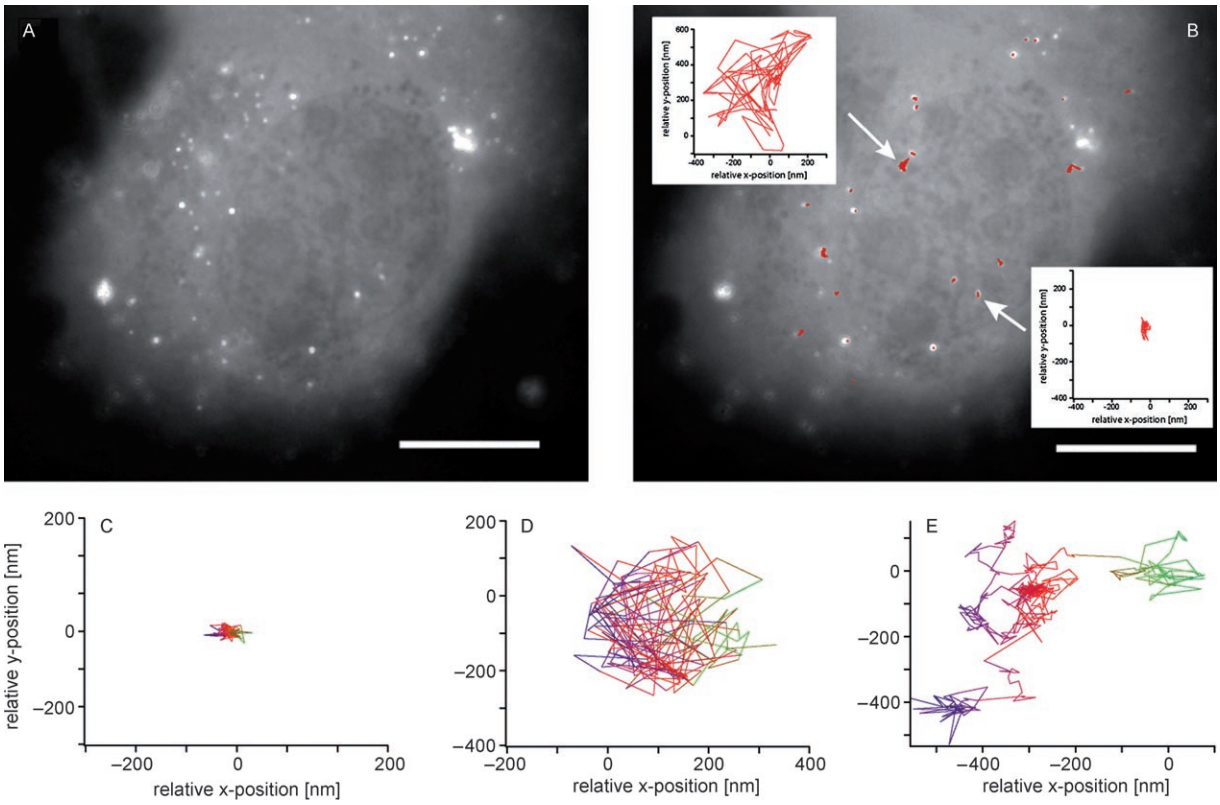

Figure 3. A) An osteoblast cell decorated with RGD-Hegas-QDs. B) After only 10 s approximately 50% of the QDs have died down. The position of the bound QDs (red trajectories) is followed in time by a tracking algorithm. Scale bars: 10 μm. C, D, E) Three qualitatively different behaviors in motion are identified. Most QDs are tightly bound (C), while a second species is only weakly bound and seems to diffuse freely within the glycocalix (D). Only a few QDs exhibit a localized diffusive motion (E). For all tracking data the starting point was set to zero; note that the same scaling was always applied. The color scheme indicates the time evolution (from green to blue).

NANO MICRO small

To address the question of whether or not any quantitative evaluation of QD tracking data is harmed by their blinking properties, we investigated the mean-square displacement (MSD)

$$\mathrm{MSD}(\tau) = \sum_i [\vec{r}(i\Delta t + \tau) - \vec{r}(i\Delta t)]^2 \quad (1)$$

of simulated two-dimensional random walks, thus $\vec{r}(t) = \begin{pmatrix} x(t) \\ y(t) \end{pmatrix}$. The MSD of a diffusing particle is a key quantity since it allows the calculation of its diffusion constant D via $\mathrm{MSD}(\tau) = D\tau$.

Due to blinking events the current coordinates of a given QD are not accessible from time to time. To deal with this complication, any tracking software has to make assumptions on the particle position during blinking. In the following, we argue that the most reasonable approach would be to assume that the particle has not moved at all during its "dark state". Thus, the calculated MSD is not altered at all by the blinking events (see Figure 4). More than 40% of all coordinates can be affected by blinking without significantly changing the calculated MSD if the overall statistics are good enough to sufficiently represent the particle motion. Besides that, one should be aware that only the first 10% of the calculated MSD data can be evaluated. Thus, the measured trajectories have to cover a timescale that is an order of magnitude higher than the timescale spanned by the MSD.

In contrast to blinking events, tracking artifacts have a strong impact on the MSD. If tracking errors occur, that is, if the image-processing software mixes up the QD position with any other bright object in close proximity during a blinking event, the resulting MSD suffers from this error. The calculated MSD curves acquire an offset, which increases with growing tracking-error probability, p_e. By accounting for this artificial offset, it is still possible to obtain an accurate value for D since the slope of the MSD is not severely affected—as long as this tracking error is moderate. However, it is crucial to note that deleting these erroneous coordinates would adulterate the time axis and thus affect D further. Finally, the worst alternative would be to assign a fixed particle position to each dark state (see also the Supporting Information). While setting these fixed coordinates to "not a number" completely prevents the calculation of the MSD, any other pair of fixed coordinates creates two artifacts at the same time. First, the MSD gains an offset again; second, the slope of the MSD decreases with respect to p_e, which results in an underestimation of the diffusion constant.

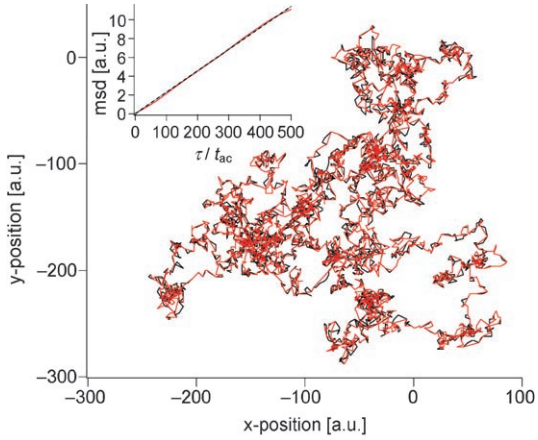

Figure 4. Two-dimensional simulation of a random walk in arbitrary units (5000 data points). The black trajectory shows the original data, and the red trajectory was created by introducing a blinking probability (p_b) of 40%. The corresponding MSDs are depicted in the inset ($p_b = 0$ and 40%) and overlay perfectly. Note that only the first 10% of the calculated MSD is shown. The time axis is given in units of the image acquisition time t_{ac}; the dashed line is a linear fit to the calculated MSDs.

3. Conclusions

We have shown that the pentapeptide cyclo(-RGDfK-) can be used to specifically label membrane integrins in living osteoblast cells with biofunctionalized QDs. For this purpose it is crucial to provide a spacer molecule of sufficient length to connect the cRGD motif and the QD surface. By following the fluorescence signal of the specifically bound QDs, the position of labeled integrins can be followed indirectly with nanometer accuracy. As revealed by our simulations, the blinking properties of QDs do not harm the quantitative evaluation of the obtained trajectories as long as the resulting lack of spatial information is handled with care. Still, the observed "QD dying" has to be investigated in more detail, since this remains the only obstacle to preventing further investigations of integrin mobility in living cells. In general, the approach we demonstrate here would be applicable to any other membrane protein that can be addressed with specific peptide sequences, provided that specific labeling is achieved.

4. Experimental Section

Materials: CdSe/ZnS QDs with an emission wavelength of 655 nm were obtained from Quantum Dot Corporation (Hayward, USA). Amino acids and coupling reagents were purchased from Novabiochem (Schwalbach) and solid-phase resin from Pepchem (Tübingen). All other chemicals were obtained from Aldrich, Acros, Sigma, or Fluka. Semipreparative high-performance liquid chromatography (HPLC) was performed on a Beckmann instrument (System Gold, solvent delivery module 126, UV detector 166) using a YMC-ODS-A 120 5-C18 column (5 μm, 20 × 250 mm^2), with a flow rate of 6 $mL\,min^{-1}$. The eluent was 0.1% trifluoroacetic acid (TFA) in various acetonitrile–water gradients. HPLC mass spectrometry (MS) analyses were performed on a Hewlett–Packard Series HP 1100 instrument. A YMC-ODS-A 120 3-C18 column (3 μm, 2 × 125 mm^2) with a flow rate of 0.3 $mL\,min^{-1}$ was used. The eluent was 0.1% formic acid in an acetonitrile–water gradient (10–50% acetonitrile in water over 15 min). Electrospray ionization (ESI) MS measurements were performed on a Finnigan LCQ instrument.

QD functionalization and integrin labeling: The design of our QD–RGD peptide system is depicted in Figure 5A. We used prefunctionalized conjugates that possessed a polymer coating to avoid toxicity and to allow active ester coupling reactions with other biomolecules, and therefore biofunctionalization. For the QDs used in this study typically five to ten streptavidin molecules were attached per QD, which resulted in QD–streptavidin conjugates with high specific biological activity.[2] Previous to our study, the coating of QDs was developed by chemical modification through covalent anchoring[25] or encapsulation by a layer of lipids[31] or polymers.[32] Here, we report the functionalization of QDs with α_v-specific integrin RGD peptides by using the biotin–streptavidin system. The biotin–streptavidin pair is the strongest noncovalent biological interaction known, with a dissociation constant, K(d), in the order of 4×10^{-14} M. The strength and specificity of the interaction has led it to be one of the most widely used affinity pairs in molecular, immunological, and cellular assays.

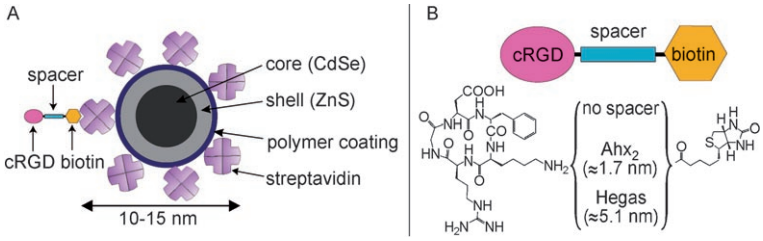

Figure 5. A) Schematic representation of the functionalization of CdSe/ZnS QDs. B) The investigated constructs with three different spacer lengths.

The distance between the RGD binding sequence and the anchoring moiety is a crucial parameter for effective integrin-mediated cell adhesion.[17] Taking this into account, three cRGD constructs, which differed in spacer length and hydrophilicity (although it was already proved that a change of the hydrophilicity normally resulted in no significant differences in cell attachment), were synthesized and tested for comparative studies (see Figure 5B and Supporting Information). Starting with constructs without a spacer (weight-average molecular weight $M_w \approx 0.8$ kDa), two molecules of Ahx served as a short spacer sequence with a length of 1.7 nm (resulting $M_w \approx 1.1$ kDa) and two molecules of Hegas (resulting $M_w \approx 1.5$ kDa) gave rise to a spacer length of ≈5.1 nm. For each spacer length a control molecule, cyclo(-RβADK-) or cyclo(-RDGfK-), was used in which the RGD sequence was replaced by a highly similar cyclic peptide sequence with much lower affinity to integrins.[33]

The RGD peptides were synthesized by derivatization of the peptide cyclo(-R(Pbf)GD(O^tBu)fK-) as described before.[18] The negative controls, cyclo(-R(Pbf)βAD(O^tBu)fK-) and cyclo(-R(Pbf)D-(O^tBu)GfK-), were prepared in a similar manner. The spacer amino acid Fmoc-Hegas-OH (20-(*N*-Fmoc)-amino-3,6,9,12,15,18-hexaoxaeicosanoic acid; Fmoc: 9-fluorenylmethoxycarbonyl) was synthesized according to Thumshirn et al.[26] The synthesis of the anchor-spacer unit was developed on a solid phase peptide synthesis (SPPS) by using a trityl chloride polystyrene (TCP) resin[34] and application of the Fmoc strategy[35] starting from *N*-Fmoc-6-aminohexanoic acid (or Fmoc-Hegas-OH), respectively. Afterwards, another *N*-Fmoc-6-aminohexanoic acid (or Fmoc-Hegas-OH) unit followed by biotin was coupled under standard peptide-coupling conditions with TBTU/HOBt/DIEA in NMP (TBTU: O-(1H-benzotriazol-1-yl)-N,N,N′,N′-tetramethyluronium-tetrafluoroborate; HOBt: 1-hydroxybenzotriazole; DIEA: diisopropylethylamine; NMP: N-methylpyrrolidone). Cleavage from the resin was accomplished with CH_2Cl_2/TFA (95:5). Fragment coupling of the anchor constructs with the partially protected peptides was carried out in dry DMF by using HATU/HOAt/collidine (1/1/10 equiv; HATU: O-(7-azabenzotriazol-1-yl)-N,N,N′,N′-tetramethyluroniumhexafluorophosphate; HOAt: 1-hydroxy-7-azabenzotriazole) as coupling reagents. For deprotection the peptides were dissolved in a mixture of 95% TFA in H_2O. After 3 h the solvent was removed under reduced pressure and the residue was precipitated in diethyl ether. Reverse-phase (RP) HPLC purification followed by lyophilization yielded the desired coating constructs as white hygroscopic powders.

For biofunctionalization the QD–streptavidin conjugates were suspended in phosphate-buffered saline (PBS; 250 μL; 8 mM Na_2HPO_4, 1.5 mM KH_2PO_4, 137 mM NaCl, 2.7 mM KCl, pH 7.4) to a final concentration of 1 nM and incubated overnight with 100 nM biotinylated peptide constructs (= 10× solution). Calvaria osteoblasts were cultured using Dulbecco's modified Eagle's medium (DMEM) containing 10% fetal bovine serum (FBS), split, and settled on sterilized glass slides in six wells at low cell density. Cells were incubated again at 37 °C and 5% CO_2 overnight in DMEM to form adhesions. The following day, the medium was removed and replaced by the QD solution (10× solution diluted 1:10 in PBS^+, that is, PBS with additional 0.9 mM $CaCl_2$, 0.5 mM $MgCl_2$, 5.5 mM glucose, pH 7.4). Overnight the cells were incubated with the QD solution to allow binding of the QD constructs to the integrins of the cell.[36] The QD density was adjusted to 0.1 nM for all experiments. Incubation was terminated the next morning by removing the QD solution and thoroughly rinsing the cells with PBS. Cells were kept in PBS^+ until used for microscopy, then PBS^+ including *N*-(2-hydroxyethyl)piperazine-*N*′-(2-ethanesulfonic acid) (HEPES; 25 mM) was used to stabilize the pH.

Image acquisition and processing: Fluorescence images were acquired on an Axiovert 200 microscope (Zeiss, Oberkochen, Germany) with a Zeiss Fluar 100× 1.3 NA oil objective and a customized filter set (excitation: bandpass 360–400 nm; beam splitter 475 nm; emission: longpass 500 nm) which allowed imaging of cell autofluorescence and QD fluorescence at the same time. Samples were illuminated by an HBO 103 W/2 mercury short-arc lamp (100 W, Osram, Germany), and images were acquired with a digital camera (ORCA-ER C4742-95, Hamamatsu, Japan) using image acquisition software developed in our group (OpenBox[22]). The QD position was followed by a tracking algorithm using a two-dimensional Gaussian fit to the QD intensity profile, which resulted in subpixel precision (< 5 nm[22]) similar to tracking methods used by other groups.[37]

Acknowledgements

We thank G. Chmel for assistance with cell culturing. Financial support by Deutsche Forschungsgemeinschaft through the DFG-Cluster of Excellence "Nanosystems Initiative Munich (NIM)" and the "Munich Center for Integrated Protein Science (CIPSM)" is gratefully acknowledged. O.L. acknowledges support from CompInt in the framework of the ENB Bayern. M.L.-G. thanks the Alexander von Humboldt Foundation for a postdoctoral fellowship.

[1] X. Michalet, F. F. Pinaud, L. A. Bentolila, J. M. Tsay, S. Doose, J. J. Li, G. Sundaresan, A. M. Wu, S. S. Gambhir, S. Weiss, *Science* **2005**, *307*, 538 – 544.
[2] QD Corporation, QD Streptavidin Conjugates User Manual, **2005**.
[3] A. R. Bausch, D. J. Weitz, *J. Nanopart. Res.* **2002**, *4*, 477 – 481.
[4] J. A. Eble in *Integrin–Ligand Interaction*, Springer, Heidelberg, **1997**, pp. 1 – 40.
[5] A. Van der Flier, A. Sonnenberg, *Cell Tissue Res.* **2001**, *305*, 285 – 298.
[6] R. O. Hynes, *Cell* **1992**, *69*, 11 – 25.
[7] M. D. Pierschbacher, E. Ruoslahti, *Nature* **1984**, *309*, 30 – 33.
[8] M. Pfaff in *Integrin–Ligand Interaction* (Ed.: J. A. Eble), Springer, Heidelberg, **1997**, pp. 101 – 121.
[9] M. Arnold, E. A. Cavalcanti-Adam, R. Glass, J. Blummel, W. Eck, M. Kantlehner, H. Kessler, J. P. Spatz, *ChemPhysChem* **2004**, *5*, 383 – 388.
[10] U. Hersel, C. Dahmen, H. Kessler, *Biomaterials* **2003**, *24*, 4385 – 4415.
[11] T. Weide, A. Modlinger, H. Kessler, *Top. Curr. Chem.* **2007**, *272*, 1 – 50.
[12] R. Haubner, D. Finsinger, H. Kessler, *Angew. Chem.* **1997**, *109*, 1440 – 1456; *Angew. Chem. Int. Ed. Engl.* **1997**, *36*, 1375 – 1389.
[13] P. Shaffner, D. Dard, *Cell. Mol. Life Sci.* **2003**, *60*, 119 – 132.
[14] R. Haubner, R. Gratias, B. Diefenbach, S. L. Goodman, A. Jonczyk, H. Kessler, *J. Am. Chem. Soc.* **1996**, *118*, 7461 – 7472.
[15] M. Friedlander, P. C. Brooks, R. W. Shaffer, C. M. Kincaid, J. A. Varner, D. A. Cheresh, *Science* **1995**, *270*, 1500 – 1502.
[16] M. Pfaff, K. Tangemann, B. Müller, M. Gurrath, G. Müller, H. Kessler, R. Timpl, J. Engel, *J. Biol. Chem.* **1994**, *269*, 20 233 – 20 238.
[17] M. Kantlehner, D. Finsinger, J. Meyer, P. Schaffner, A. Jonczyk, B. Diefenbach, B. Nies, H. Kessler, *Angew. Chem.* **1999**, *111*, 587 – 590; *Angew. Chem. Int. Ed.* **1999**, *38*, 560 – 562.
[18] M. Kantlehner, P. Schaffner, D. Finsinger, J. Meyer, A. Jonczyk, B. Diefenbach, B. Nies, G. Holzemann, S. L. Goodman, H. Kessler, *ChemBioChem* **2000**, *1*, 107 – 114.
[19] B. Hu, D. Finsinger, K. Peter, Z. Guttenberg, M. Bärmann, H. Kessler, A. Escherich, L. Moroder, J. Bohm, W. Baumeister, S. F. Sui, E. Sackmann, *Biochemistry* **2000**, *39*, 12 284 – 12 294.
[20] Z. Guttenberg, A. R. Bausch, B. Hu, R. Bruinsma, L. Moroder, E. Sackmann, *Langmuir* **2000**, *16*, 8984 – 8993.
[21] J. J. Calvete, *Cell Adhesion Molecules*, Plenum, New York, **1993**.
[22] J. Schilling, E. Sackmann, A. R. Bausch, *Rev. Sci. Instrum.* **2004**, *75*, 2822 – 2827.
[23] D. Marsh, L. I. Horvath, *Biochim. Biophys. Acta Rev. Biomembr.* **1998**, *1376*, 267 – 296.
[24] S. K. Akiyama, E. Hasegawa, T. Hasegawa, K. M. Yamada, *J. Biol. Chem.* **1985**, *260*, 13 256 – 13 260.
[25] W. Cai, D.-W. Shin, K. Chen, O. Gheysens, Q. Cao, S. X. Wang, S. S. Gambhir, X. Chen, *Nano Lett.* **2006**, *6*, 669 – 676.
[26] G. Thumshirn, U. Hersel, S. L. Goodman, H. Kessler, *Chem. Eur. J.* **2003**, *9*, 2717 – 2725.
[27] E. Garanger, D. Boturyn, J.-L. Coll, M.-C. Favrot, P. Dumy, *Org. Biomol. Chem.* **2006**, *4*, 1958 – 1965.
[28] L. L. Kiessling, J. E. Gestwicki, L. E. Strong, *Angew. Chem.* **2006**, *118*, 2408 – 2429; *Angew. Chem. Int. Ed.* **2006**, *45*, 2348 – 2368.
[29] M. Nirmal, L. Brus, *Acc. Chem. Res.* **1999**, *32*, 407 – 414.
[30] X. Michalet, F. Pinaud, T. D. Lacoste, M. Dahan, M. P. Bruchez, A. P. Alivisatos, S. Weiss, *Single Mol.* **2001**, *2*, 261 – 276.
[31] W. J. M. Mulder, R. Koole, R. J. Brandwijk, G. Storm, P. T. K. Chin, G. J. Strijkers, C. de Mello Donega, K. Nicolay, A. W. Griffioen, *Nano Lett.* **2006**, *6*, 1 – 6.
[32] X. Y. Wu, H. J. Liu, J. Q. Liu, K. N. Haley, J. A. Treadway, J. P. Larson, N. F. Ge, F. Peale, M. P. Bruchez, *Nat. Biotechnol.* **2003**, *21*, 41 – 46.
[33] The IC_{50} value for the RGD sequence is three orders of magnitude lower than the corresponding value of the control molecules.
[34] K. Barlos, D. Gatos, J. Kallitsis, G. Papaphotiu, P. Sotiriu, W. Q. Yao, W. Schafer, *Tetrahedron Lett.* **1989**, *30*, 3943 – 3946.
[35] G. B. Fields, R. L. Noble, *Int. J. Pept. Protein Res.* **1990**, *35*, 161 – 214.
[36] A shorter incubation with the QD solution for 1 h did not change the results..
[37] M. Dahan, S. Levi, C. Luccardini, P. Rostaing, B. Riveau, A. Triller, *Science* **2003**, *302*, 442 – 445.

Received: February 2, 2007
Revised: June 4, 2007
Published online on August 20, 2007

